IEEE Access
Multidisciplinary | Rapid Review | Open Access Journal

Received November 15, 2018, accepted December 3, 2018, date of publication December 19, 2018,
date of current version January 16, 2019.

Digital Object Identifier 10.1109/ACCESS.2018.2888630

A Novel Region-Refinement Pulse Width Modulation Method for Torque Ripple Reduction of Brushless DC Motors

KAI LIU, ZHIQIANG ZHOU, AND WEI HUA, (Senior Member, IEEE)
School of Electrical Engineering, Southeast University, Nanjing 210096, China

Corresponding author: Wei Hua (huawei1978@seu.edu.cn)

This work was supported in part by the National Key R&D Programme of China under Grant 2017YFB1300900, and in part by the National Natural Science Foundation of China under Grant 51777032.

ABSTRACT Brushless dc motors (BLDCMs) exhibit relatively large torque ripple due to the current pulsation during the commutation process. In this paper, first, the production mechanism of the commutation torque ripple is analyzed in detail, where the diode freewheeling in the inactive phase winding and the non-commutation torque ripple under the existing PWM modulation modes are compared for a three-phase six-switch inverter-fed BLDCM drive. The torque ripple expression of each PWM mode is derived analytically. Thereafter, a new region-refinement PWM method is proposed, in which a normal operation region of 60° is refined into two 30° sub-regions, and PWM-ON and ON-PWM modulation method is suitable to be employed, respectively, in the former and latter 30° regions. To verify the effectiveness of reducing the non-commutation torque ripple, both simulations and experiments are conducted on a three-phase prototyped BLDCM. The results demonstrate that the torque ripple under the proposed PWM mode can be reduced significantly.

INDEX TERMS Brushless dc motors, pulse width modulation, torque ripple reduce.

I. INTRODUCTION

Brushless DC motors (BLDCMs) with trapezoidal phase back-EMF waveform have received a great deal of attention in many industrial applications, owing to its simple structure, high power density, high reliability, and low cost. Therefore, it is widely applied in office automation, computer peripheral devices and instruments, as well as domestic electric appliances, etc. [1]. However, in a practical BLDCM-based drive, significant torque pulsations may arise due to the imperfect back-EMF waveform, commutation modes between phase windings, and cogging torque, etc. [2]–[5]. Particularly, caused by the freewheeling of phase currents and limited DC-link bus voltages, the torque ripple during phase current commutation is usually considered as one of the main drawbacks of BLDCM drives, which varies with different PWM modes [6]–[8]. In addition, the non-commutation phase current as well as the output torque may also fluctuate significantly in the course of commutation period [9]. Consequently, the unfavourable vibration and noise due to commutation torque ripple restrict the application of BLDCMs in high-precision servo systems [10]. Therefore, reducing the commutation torque ripple is of great significance in expanding application fields of BLDCMs.

Recently, torque ripple reduction of BLDCMs has been the research focus, and the ongoing works are concentrated on the torque ripple component due to commutation and the torque ripple component produced as a result of diode freewheeling of non-conducting phase. In [11], the commutation torque ripple was regarded as independent of current and varies with rotation speeds, and it could even reach 50% of the averaged electromagnetic torque. In [12], a Buck converter was introduced to control the DC-link voltage to decrease the commutation torque ripple, but the bandwidth of converter was not taken into consideration, hence it was only suitable for low speed operation. In [13], a SEPIC-based circuit was used, but this structure has to add three switches, and their respective inductances, capacitances, and diodes, which increases the complexity of the control system. On the other hand, the influences of four traditional PWM patterns on the commutation torque ripples were investigated and the PWM-ON mode was selected as the best one to produce the smallest torque ripple for BLDCMs in [14]. Moreover, in [15] the effect of PWM modes on the non-commutation torque ripple was analyzed, but the case during commutation was not considered.

A new method called PWM-ON-PWM was carried out in [16], where the focus is on the characteristics of diode freewheeling, and it proved that the method proposed can eliminate the diode freewheeling completely. In [17] and [18], for the diode freewheeling of non-conducting phase

windings, the modulation schemes, including PWM_ON _PWM and PWM_PWM, were investigated, and hence the diode freewheeling of non-commutation phase could be reduced.

Based on the above analysis, it can be concluded that PWM_ON_PWM is an efficient modulation pattern from the viewpoint of power loss. However, almost all the articles that discuss PWM-ON-PWM method were focused only on the reduction of torque ripple through controlling the current of diode freewheeling by experiments, and the theoretical derivation and control guidance of PWM_ON_PWM mode are unavailable.

Overall, it is found from the previous literatures that PWM modulation methods play a significant role in the production and suppression of undesired torque ripples. Hence, rigorous theory derivation of the influence of PWM modulation modes on the commutation torque ripple is conducted firstly in this paper. Then, according to the derived results, a novel PWM mode is proposed to reduce torque ripple, which splits each commutation period 60° in electrical degrees for a conventional three-phase BLDCM) into two refined regions, and the former 30° and latter 30° are controlled differently.

The remainder of this paper is organized as follows. Section 2 investigates the influence of different PWM modes with detailed theory derivations on torque ripple. Then, based on the results in Section 2, a new region-refinement PWM method is proposed based on the principle of torque ripple minimization in Section 3. Thereafter, both simulations and experimental verifications on a prototyped BLDCM are performed in Section 4, and the results confirm the effectiveness of the method. Finally, conclusions are drawn in Section 5.

II. INFLUENCE OF PWM MODES ON TORQUE RIPPLE

Fig. 1(a) shows the equivalent model of a three-phase BLDCM-based drive system, where the BLDCM is star-type connected and fed by a conventional three-phase voltage source inverter (VSI). U_s is the DC-bus voltage, V_1 ~V_6 are the power switches, usually being IGBTs or MOSFETs, VD_1 ~VD_6 are the freewheel diodes, and U_N is the voltage of neutral point connecting three-phase windings. Ideally, a BLDCM is conventionally fed by standard rectangular currents, so the produced electromagnetic torque is theoretically constant. Fig. 1(b) shows the six sectors of space voltage vectors of a 3-phase BLDCM. Fig. 1(c) shows the ideal three-phase back-EMFs and currents waveforms of a BLDCM.

Fig. 2 shows the schematic diagrams of traditional four single-edge PWM modes, where single-edge means only upper-bridge or lower-bridge employs chopping modulation in any 60ř sectors. As shown in Fig. 2, an electrical cycle (360°) is normally divided into six regions, and every region covers 60° in electrical degrees. The areas of square-pulse waves stand for the regions employing PWM chopping. Taking Fig. 2(a) as an example, for each power switch (V_1 ~V_6), the PWM modulation will last 60° after the corresponding transistor turns on, and then the transistor keeps the turn-on status for another 60° degrees before it turns off in a

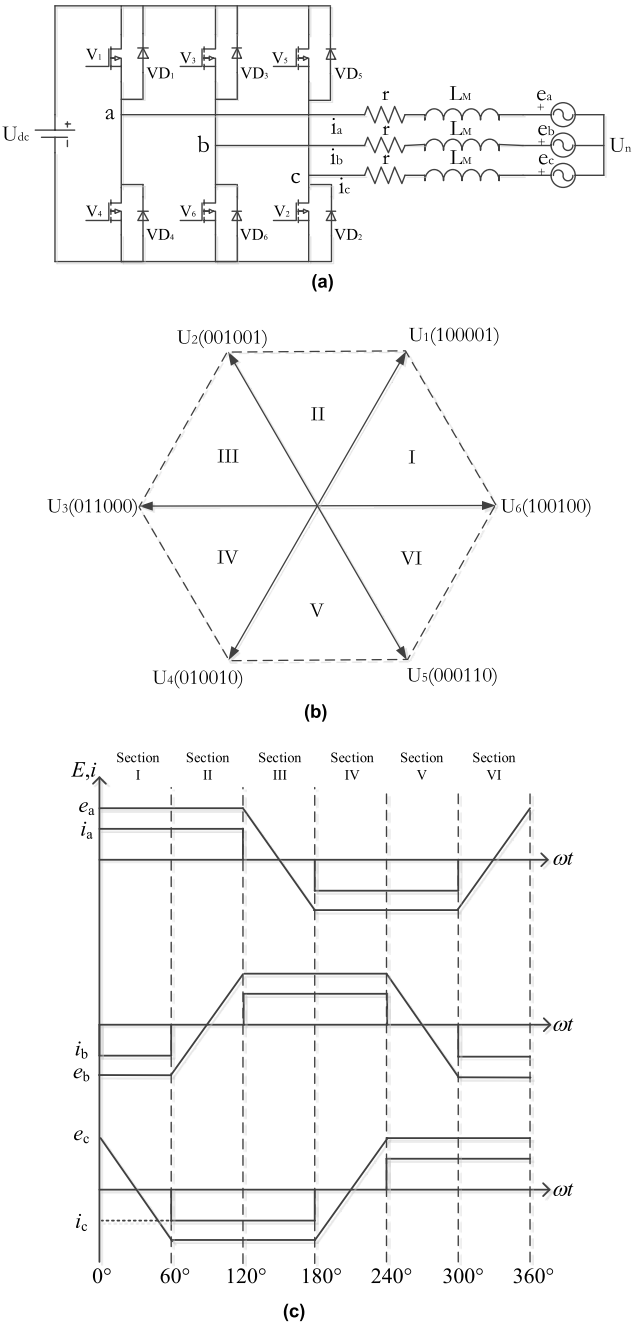

FIGURE 1. The configuration, space sectors distributions and ideal three-phase back-EMFs and currents waveforms of a 3-phase BLDCM. (a) The equivalent circuit of a 3-phase BLDCM. (b) The six sectors of space voltage vectors of a 3-phase BLDCM. (c) Ideal three-phase back-EMFs and currents waveforms of a BLDCM.

whole electric cycle (360°). Hence, such a modulation mode is called as "PWM-ON". In contrary, if the PWM chopping region and the constant turn-on region is reversed as shown in Fig. 2(b), it is named as "ON-PWM", where the turn-on status is firstly kept during the former 60° region, and then the PWM chopping is applied in the latter 60° region. However, as for Fig. 2(c), the PWM modulation is only used in the upper-bridge (V_1, V_3, V_5) and will last 120° electrical angles. Meanwhile, the corresponding power switch of the

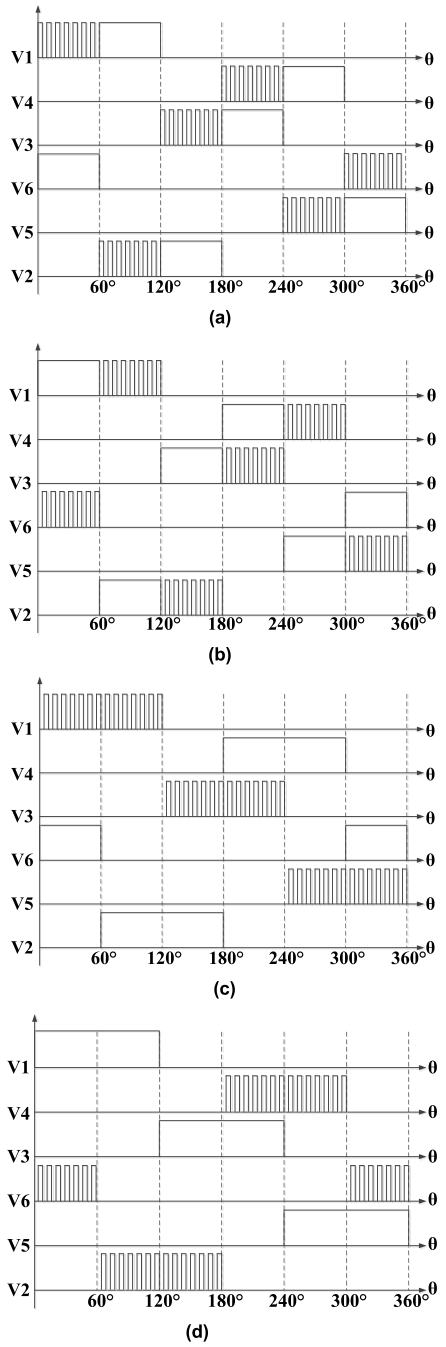

FIGURE 2. Schematic diagrams of traditional four PWM modes for BLDCMs. (a) PWM-ON mode. (b) ON-PWM mode. (c) H_PWM-L_ON. (d) H_ON-L_PWM mode.

lower-bridge (V_4, V_6, V_2) keeps turn-on status for 120° electric angles in a whole electric cycle (360°). Hence, such a modulation mode is called as ''H_PWM-L_ON''. Similarly, the fourth mode is ''H_ON-L_PWM'' as shown in Fig. 2(d).

A. IDEAL ELECTROMAGNETIC TORQUE IN STEADY STATE

According to the fundamental operation principle shown in Fig. 1(c), a complete electrical period of 360° is divided into six sectors, and the phase back-EMF waveform cooperates with the phase current waveform. Then, the synthesis of three-phase electromagnetic torque T_e of a BLDCM is expressed by equation (1):

$$T_e = \frac{n_p}{\omega}(e_a i_a + e_b i_b + e_c i_c) \tag{1}$$

where, n_p is rotor pole-pair number, ω is the mechanical rotation speed (rad/s), $e_a/e_b/e_c$ and $i_a/i_b/i_c$ are the three-phase back-EMF and armature currents, respectively.

Under ideal condition, the H_PWM-L_ON mode schematic diagram in the commutation process from section II to sector III is chosen as an example for analysis. At the beginning of the commutation, V_1 closes and V_3 opens, and the initial values of three-phase currents have to satisfy the constraint that $i_a = 0$, $i_b = i_0$, $i_c = -i_0$, where i_0 is the steady phase current of the BLDCM at a certain speed. At this time, the corresponding electromagnetic torque can be expressed as

$$T_e = \frac{n_p}{\omega}(e_b i_b + e_c i_c) \tag{2}$$

Meanwhile, $e_b = k_e\omega$, $e_c = -k_e\omega$, and equation (2) can be simplified as

$$T_e = \frac{n_p}{\omega}(e_b i_b + e_c i_c) = 2n_p k_e i_0 = T_0 \tag{3}$$

where, k_e is the back-EMF constant (V per rad/s), and T_0 is the ideally steady electromagnetic torque of the BLDCM.

B. INFLUENCE OF PWM METHODS ON COMMUTATIONS

According to equation (3), the ideal electromagnetic torque T_0 is unchanged when i_0 remains constant. Therefore, BLDCM exhibits the same mechanical properties, such as the torque-speed curve, like a brush DC motor. However, when the motor operates in the commutation periods, hysteresis exists in the converter process because of the armature inductance, where the power switches cannot behave like the ideal switches and both the turn-on and turn-off phase currents needs time to grow up to the constant value or decay to zero. In the case of the commutation process from sector II to sector III, i_a cannot decrease to zero immediately but gradually, and meanwhile, i_b gradually increase to i_0. During this commutation, the corresponding three-phase voltages satisfy equation (4). The detailed derivation can be found in table 5 in appendices.

$$\begin{cases} e_a = -\dfrac{6}{\pi}k_e\omega^2 t + k_e\omega \\ e_b = k_e\omega \\ e_c = -k_e\omega \end{cases} \tag{4}$$

As shown in Table 1, when in upper-bridge current commutation, PWM_ON and H_PWM-L_ON share the same modulation method, while ON_PWM and H_ON-L_PWM share the same. When in lower-bridge current commutation, ON_PWM and H_PWM-L_ON employ the same modulation method, whereas PWM_ON and H_ON-L_PWM share the same. In the followings, detailed influence of PWM modes on torque ripple will be analytically derived and evaluated.

TABLE 1. Phase modulation method during commutation.

Modulation method	Upper-bridge current commutation (Sectors I, III, V)		Lower-bridge current commutation (Sectors II, IV, VI)	
	upcoming phase	non-commutation phase	upcoming phase	non-commutation phase
PWM_ON	PWM modulation	open	PWM modulation	open
ON_PWM	open	PWM modulation	open	PWM modulation
H_PWM-L_ON	PWM modulation	open	open	PWM modulation
H_ON-L_PWM	open	PWM modulation	PWM modulation	open

C. MODULATION METHODS ON TORQUE RIPPLE

1) UPPER-BRIDGE CURRENT COMMUTATION

a: PWM-ON and H_PWM-L_ON

Firstly, the cases of PWM-ON and H_PWM-L_ON modes during the commutation process from sector II to sector III are taken as examples, where the power switch V_1 turns off, and V_3 turns on the PWM mode simultaneously, as well as V_2 keeps the open status. The current loop of phase A in the course of freewheeling is highlighted in Fig. 3. It can be found that the current path of phase B is different when the status of V_3 is changed from turn-on to turn-off.

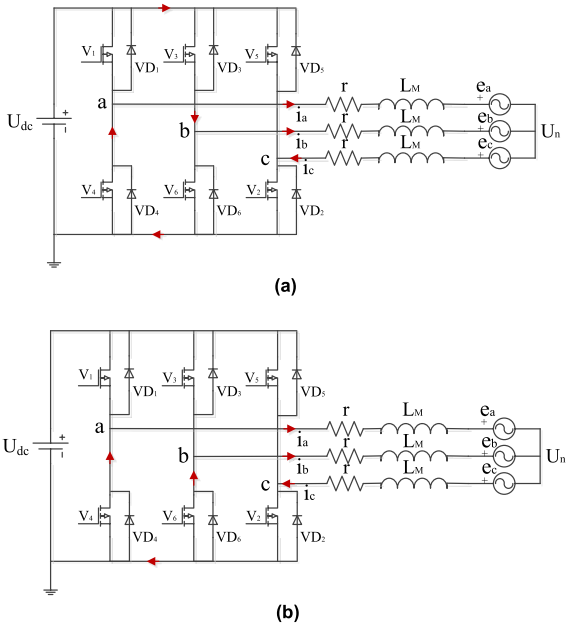

FIGURE 3. PWM-ON and H_PWM-L_ON methods in upper-bridge current commutation. (a) when V3 turns on. (b) when V3 turns off.

Correspondingly, the three-phase voltage equations in the freewheeling process of phase A yield [19-21]:

$$\begin{cases} Ri_a + \dfrac{di_a}{dt} + e_a + U_n = 0 \\ Ri_b + \dfrac{di_b}{dt} + e_b + U_n = SU_{dc} \\ Ri_c + \dfrac{di_c}{dt} + e_c + U_n = 0 \end{cases} \tag{5}$$

where, R is the phase resistance, L is the phase inductance, $e_a/e_b/e_c$ and $i_a/i_b/i_c$ are the three-phase back-EMFs and armature currents. $S = 0$ or 1, whose value depends on the switching function of V_3, i.e., V_3 is on, $S = 1$; V_3 is off, $S = 0$.

Consequently, the neutral point voltage U_n can be obtained by adding the three above equations:

$$U_n = \begin{cases} \dfrac{1}{3}U_{dc} - \dfrac{1}{3}\sum_{i=a,b,c} e_i & S = 1 \\ -\dfrac{1}{3}\sum_{i=a,b,c} e_i & S = 0 \end{cases} \tag{6}$$

It should be noted that during the commutation process from sectors II to III, the three-phase back-EMFs yield equation (4).

Defining the electrical time constant of the BLDCM is $\tau = \frac{L}{R}$, the carrier cycle of PWM is T_s, and the current PWM duty cycle is D, and considering normally $\frac{T_s}{\tau} \ll 1$, U_n can take an approximated treatment as:

$$U_n = \frac{D}{3}U_{dc} - \frac{1}{3}e_a \tag{7}$$

Substituting equation (7) into equation (5), it can be obtained,

$$\begin{cases} \dfrac{di_a}{dt} + \dfrac{1}{\tau}i_a = -\dfrac{1}{3L}(2k_e\omega + DU_{dc}) + \dfrac{4}{\pi L}k_e\omega^2 t = k_0 + k_1 t \\ \dfrac{di_b}{dt} + \dfrac{1}{\tau}i_b = \dfrac{2}{3L}(DU_{dc} - k_e\omega) - \dfrac{2}{\pi L}k_e\omega^2 t = k_2 + k_3 t \\ \dfrac{di_c}{dt} + \dfrac{1}{\tau}i_c = \dfrac{1}{3L}(4k_e\omega - DU_{dc}) - \dfrac{2}{\pi L}k_e\omega^2 t = k_4 + k_3 t \end{cases} \tag{8}$$

where

$$\begin{cases} k_0 = -\dfrac{1}{3L}(2k_e\omega + DU_{dc}) \\ k_1 = \dfrac{4}{\pi L}k_e\omega^2 \\ k_2 = \dfrac{2}{3L}(DU_{dc} - k_e\omega) \\ k_3 = \dfrac{2}{3L}(DU_{dc} - k_e\omega) \\ k_4 = \dfrac{1}{3L}(4k_e\omega - DU_{dc}) \end{cases} \tag{9}$$

Further, the initial conditions of three-phase currents before commutation satisfy: $i_a(0) = -i_c(0) = i_0$, and $i_b(0) = 0$.

Substituting the initial values of three-phase currents into equation (8) and employing Laplace Transform, the three-phase currents are be transformed as:

$$\begin{cases} i_a(t) = \tau k_0 - \tau^2 k_1 + \tau k_1 t + [i_0 + \tau^2 k_1 - \tau k_0] e^{-\frac{t}{\tau}} \\ i_b(t) = \tau k_2 - \tau^2 k_3 + \tau k_3 t + \left[\tau^2 k_3 - \tau k_2\right] e^{-\frac{t}{\tau}} \\ i_c(t) = \tau k_4 - \tau^2 k_3 + \tau k_3 t + [\tau^2 k_3 - \tau k_4 - i_0] e^{-\frac{t}{\tau}} \end{cases} \tag{10}$$

Consequently, the electromagnetic torque in upper-bridge current commutation can be calculated as

$$\begin{aligned} T_{upper} &= \frac{n_p}{\omega}(e_a i_a + e_b i_b + e_c i_c) \\ &= n_p\{k_e[\tau(k_0 + k_2 - k_4) - \tau^2 k_1] \\ &\quad + \left[k_e \tau k_1 - \frac{6}{\pi} k_e \omega(\tau k_0 - \tau^2 k_1)\right] t \\ &\quad + k_e \left[\tau^2 k_1 + \tau(k_4 - k_0 - k_2) + 2i_0\right] e^{-\frac{t}{\tau}} \\ &\quad - \frac{6}{\pi} k_e \omega(\tau^2 k_1 - \tau k_0 + i_0) t e^{-\frac{t}{\tau}} \\ &\quad - \frac{6}{\pi} k_e \omega \tau k_1 t^2\} \end{aligned} \tag{11}$$

As can be seen, the resultant torque formula is complex though it can describe the transient change. In the followings, a relatively practical simplification process is conducted.

As is well known from the fundamental automatic control system, when $\left|-\frac{t}{\tau}\right| \leq 0.4$, $e^{-\frac{t}{\tau}}$ can be approximately regarded as $1 - \frac{t}{\tau}$, and the induced error is within 10%. Based on the above analysis, equation (10) is simplified as:

$$\begin{cases} i_a(t) = i_0 - \dfrac{2k_e\omega + 3Ri_0 + DU_{dc}}{3L} t \\ i_b(t) = \dfrac{2}{3L}(DU_{dc} - k_e\omega)\, t \\ i_c(t) = -i_0 + \dfrac{4k_e\omega + 3Ri_0 - DU_{dc}}{3L} t \end{cases} \tag{12}$$

Considering three-phase back-EMF expressions as equation (4), and combining the back-EMFs and armature currents, the corresponding electromagnetic torque in upper-bridge current commutation is:

$$\begin{aligned} T_{upper} &= \frac{n_p}{\omega}(e_a i_a + e_b i_b + e_c i_c) \\ &= -\frac{2k_e n_p(3\pi R i_0 - \pi D U_{dc} + 4\pi k_e \omega + 9L i_0 \omega)}{3\pi L} t \\ &\quad + 2n_p k_e i_0 + \frac{2k_e n_p \omega(3Ri_0 + 2k_e\omega + DU_{dc})}{\pi L} t^2 \end{aligned} \tag{13}$$

As a sequence, the resultant torque ripple under upper-leg current commutation T_{u1} is:

$$\begin{aligned} \Delta T_{u1} &= T_0 - T_{upper} \\ &= \frac{2k_e n_p(3\pi R i_0 + 4\pi k_e \omega + 9L i_0 \omega - \pi D U_{dc})}{3\pi L} t \\ &\quad - \frac{2k_e n_p \omega(3Ri_0 + 2k_e\omega + DU_{dc})}{\pi L} t^2 \end{aligned} \tag{14}$$

b: ON-PWM and H_ON-L_PWM

Then, for ON-PWM and H_ON-L_PWM modes, like the case of PWM-ON and H_PWM-L_ON, during the commutation process from sector II to sector III, where the power switch V_1 turns off, and V_2 turns on the PWM mode simultaneously, as well as V_3 keeps the open status. The current loop of phase A in the course of freewheeling is highlighted in Fig. 4.

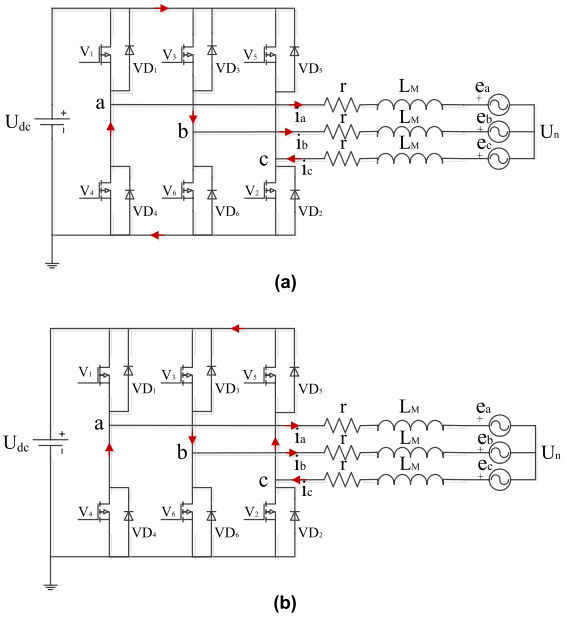

FIGURE 4. ON-PWM and H_ON-L_PWM methods in upper-bridge current commutation. (a) when V2 turns on. (b) when V2 turns off.

Correspondingly, three-phase voltages in the freewheeling course of phase A are:

$$\begin{cases} Ri_a + L\dfrac{di_a}{dt} + e_a + U_n = 0 \\ Ri_b + L\dfrac{di_b}{dt} + e_b + U_n = U_{dc} \\ Ri_c + L\dfrac{di_c}{dt} + e_c + U_n = S' U_{dc} \end{cases} \tag{15}$$

where $S' = 0$ or 1, whose value depends on the switching function of V_3. If V_3 is on, $S' = 0$; Then V_3 is off, $S' = 1$.

The neutral point voltage U_n can be obtained by adding those three equations:

$$U_n = \frac{2 - D}{3} U_{dc} - \frac{1}{3} e_a \tag{16}$$

Similarly, repeat the process for Equation (6)~Equation (12), and the three-phase currents are:

$$\begin{cases} i_a(t) = i_0 - \dfrac{2k_e\omega + 3Ri_0 + (2 - D)\, U_{dc}}{3L} t \\ i_b(t) = \dfrac{1}{3L}((1 + D)\, U_{dc} - 2k_e\omega)\, t \\ i_c(t) = -i_0 + \dfrac{4k_e\omega + 3Ri_0 + (1 - 2D) U_{dc}}{3L} t \end{cases} \tag{17}$$

As a result, the torque ripple under upper-leg current commutation T_{u2} is:

$$\begin{aligned}\Delta T_{u2} &= T_0 - T_{upper} \\ &= \frac{2k_e n_p(3\pi Ri_0 + 4\pi k_e\omega + 9Li_0\omega + (1-2D)\pi U_{dc})}{3\pi L}t \\ &\quad - \frac{2k_e n_p\omega(3Ri_0 + 2k_e\omega + (2-D)U_{dc})}{\pi L}t^2 \end{aligned} \tag{18}$$

2) LOWER-BRIDGE CURRENT COMMUTATION

a: ON-PWM and H_PWM-L_ON

As for lower-bridge current commutation, the cases of ON-PWM and H_PWM-L_ON modes during the commutation process from sector V to sector VI are taken as examples, where the power switch V_4 turns off, and V_5 turns on the PWM mode simultaneously, as well as V_6 keeps the open status. The current loop of phase A in the course of freewheeling is highlighted in Fig. 5.

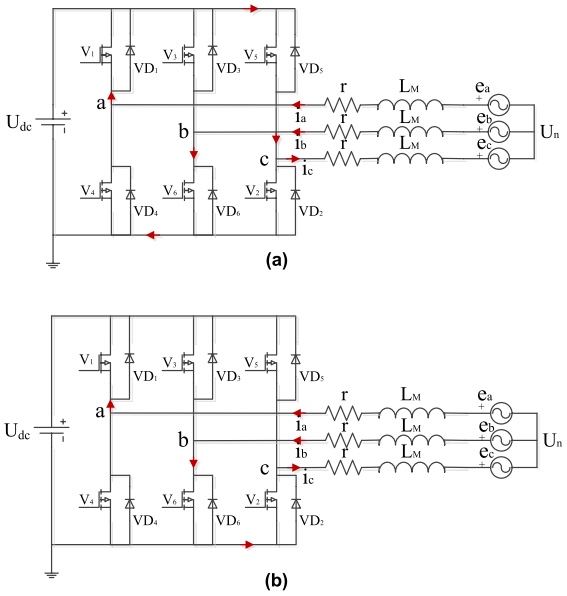

FIGURE 5. ON-PWM and H_PWM-L_ON methods in lower-bridge current commutation. (a) when V5 turns on. (b) when V5 turns off.

Correspondingly, the three-phase voltages in the freewheeling course of phase A is:

$$\begin{cases} Ri_a + L\dfrac{di_a}{dt} + e_a + U_n = U_{dc} \\ Ri_b + L\dfrac{di_b}{dt} + e_b + U_n = 0 \\ Ri_c + L\dfrac{di_c}{dt} + e_c + U_n = SU_{dc} \end{cases} \tag{19}$$

where S = 0 or 1, depending on the switching function of V_5. namely, V_5 is on, S = 1; V_5 is off, S = 0.

The neutral point voltage U_n can be obtained by adding those three equations:

$$U_n = \frac{1+D}{3}U_{dc} - \frac{1}{3}e_a \tag{20}$$

Again, based on the procedure as illustrated by equations (6) (12), the relative three-phase currents yield:

$$\begin{cases} i_a(t) = -i_0 + \dfrac{2k_e\omega + 3Ri_0 + (2-D)U_{dc}}{3L}t \\ i_b(t) = \dfrac{1}{3L}(2k_e\omega - (1+D)U_{dc})t \\ i_c(t) = i_0 + \dfrac{(2D-1)U_{dc} - 4k_e\omega - 3Ri_0}{3L}t \end{cases} \tag{21}$$

Define T_{lower} is the corresponding electromagnetic torque in lower-bridge current commutation. The torque ripple under lower-leg current commutation T_{l1} is:

$$\begin{aligned}\Delta T_{l1} &= T_0 - T_{lower} \\ &= \frac{2k_e n_p(3\pi Ri_0 + 4\pi k_e\omega + 9Li_0\omega + \pi(1-2D)U_{dc})}{3\pi L}t \\ &\quad - \frac{2k_e n_p\omega(3Ri_0 + 2k_e\omega + (2-D)U_{dc})}{\pi L}t^2 \end{aligned} \tag{22}$$

b: PWM-ON and H_ON-L_PWM

Finally, for PWM-ON and H_ON-L_PWM modes, during the commutation process from sector V to sector VI, where the power switch V_4 turns off, and V_6 turns on the PWM mode simultaneously, as well as V_5 keeps the open status. The freewheeling current loop of phase A is shown in Fig. 6.

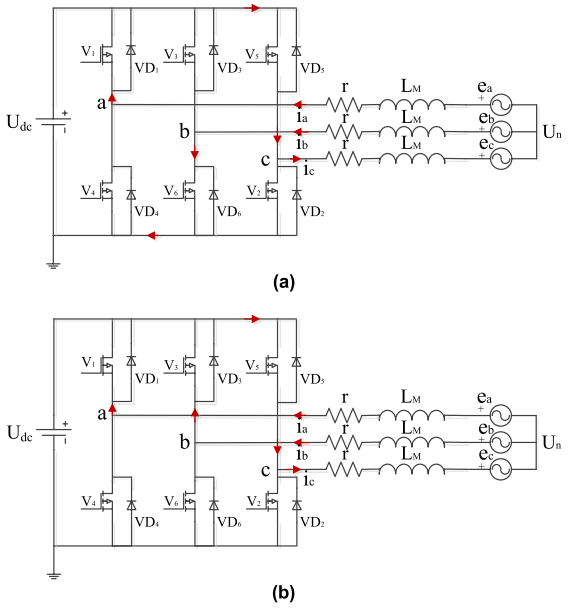

FIGURE 6. PWM-ON and H_ON-L_PWM methods in lower-bridge current commutation. (a) when V6 turns on. (b) when V6 turns off.

Correspondingly, three-phase voltage equation during the freewheeling of phase A is:

$$\begin{cases} Ri_a + L\dfrac{di_a}{dt} + e_a + U_n = U_{dc} \\ Ri_b + L\dfrac{di_b}{dt} + e_b + U_n = S'U_{dc} \\ Ri_c + L\dfrac{di_c}{dt} + e_c + U_n = U_{dc} \end{cases} \tag{23}$$

where $S' = 0$ or 1, whose value depends on the switching function of V_6 (V_6 is on, $S' = 0$; V_6 is off, $S' = 1$).

The neutral point voltage U_n can be obtained by adding those three equations:

$$U_n = \frac{3-D}{3}U_{dc} - \frac{1}{3}e_a \tag{24}$$

Similarly, repeating the process of Eq.(6)∼Eq.(12), the three-phase currents are:

$$\begin{cases} i_a(t) = -i_0 + \dfrac{2k_e\omega + 3Ri_0 + DU_{dc}}{3L}t \\ i_b(t) = \dfrac{2}{3L}(k_e\omega - DU_{dc})\,t \\ i_c(t) = i_0 + \dfrac{DU_{dc} - 4k_e\omega - 3Ri_0}{3L}t \end{cases} \tag{25}$$

The torque ripple under lower-leg current commutation T_{l2} is:

$$\begin{aligned} \Delta T_{l2} &= T_0 - T_{lower} \\ &= \frac{2k_e n_p(3\pi Ri_0 + 4\pi k_e\omega + 9Li_0\omega - \pi DU_{dc})}{3\pi L}t \\ &\quad - \frac{2k_e n_p\omega(3Ri_0 + 2k_e\omega + DU_{dc})}{\pi L}t^2 \end{aligned} \tag{26}$$

D. TORQUE RIPPLES UNDER PWM MODES

Based on the above derivations of analytical expression of torque ripple for four typical PWM modes, a comprehensive comparison can be conducted as listed in Table 2. It can be found that the torque ripple is and is a quadratic function of time t and influenced by back electromotive force (back-EMF) constant k_e, rotor pole pairs n_p, steady phase current i_0, duty ratio D, DC-link bus voltage U_{dc}, armature winding inductance L, and motor speed ω. Each torque ripple equation under different PWM modes are composed of two components, and for each component similar constituent elements exist, such as ($3\pi Ri_0$+$4\pi k_e\omega$+$9Li_0\omega$) and ($3Ri_0$+$2k_e\omega$). The difference between the four equations is mainly caused by the utilization ratio of DC-linkage voltage due to PWM modes. As a consequence, a new region-refinement PWM mode is proposed in the next section.

III. NEW REGION-REFINEMENT PWM MODE

According to the analytical expressions of the torque ripple under four PWM modes, for the case of upper-bridge current commutation, the difference of torque ripple between PWM-ON (H_PWM-L_ON) and ON-PWM (H_ON-L_PWM) can be obtained by

$$\Delta T_1 = \Delta T_{u1} - \Delta T_{u2} = -(\frac{\pi}{3} - 2\omega t)\cdot(1-D)\cdot\frac{2k_e n_p U_{dc}t}{\pi L} \tag{27}$$

It is obvious that T_1 is strongly related to ωt, namely,

$$\begin{cases} \Delta T_1 \le 0, & 0 \le \omega t \le \dfrac{\pi}{6} \\ \Delta T_1 > 0, & \dfrac{\pi}{6} < \omega t \le \dfrac{\pi}{3} \end{cases} \tag{28}$$

TABLE 2. Comparison of PWM modes on torque ripple.

upper-bridge current commutation	
PWM-ON H_PWM-L_ON	$\Delta T_{u1} = \frac{2k_e n_p(3\pi Ri_0 + 4\pi k_e\omega + 9Li_0\omega - \pi DU_{dc})}{3\pi L}t - \frac{2k_e n_p\omega(3Ri_0 + 2k_e\omega + DU_{dc})}{\pi L}t^2$
ON-PWM H_ON-L_PWM	$\Delta T_{u2} = \frac{2k_e n_p(3\pi Ri_0 + 4\pi k_e\omega + 9Li_0\omega + (1-2\mathrm{D})\pi U_{dc})}{3\pi L}t - \frac{2k_e n_p\omega(3Ri_0 + 2k_e\omega + (2-D)\ U_{dc})}{\pi L}t^2$
lower-bridge current commutation	
PWM-ON H_ON-L_PWM	$\Delta T_{l1} = \frac{2k_e n_p(3\pi Ri_0 + 4\pi k_e\omega + 9Li_0\omega + \pi(1-2\mathrm{D})U_{dc})}{3\pi L}t - \frac{2k_e n_p\omega(3Ri_0 + 2k_e\omega + (2-D)\ U_{dc})}{\pi L}t^2$
ON-PWM H_PWM-L_ON	$\Delta T_{l2} = \frac{2k_e n_p(3\pi Ri_0 + 4\pi k_e\omega + 9Li_0\omega - \pi\,\mathrm{D}U_{dc})}{3\pi L}t - \frac{2k_e n_p\omega(3Ri_0 + 2k_e\omega + DU_{dc})}{\pi L}t^2$

Equation (28) means that when operating at upper-bridge current commutation, the region of 60° ($\pi/3$) can be refined into two sub-regions, i.e., the former 30° [0, $\pi/6$] and the latter 30° [$\pi/6$, $\pi/3$]. When operated in the former 30° region, minimum torque ripple can be achieved by employing PWM_ON or H_PWM-L_ON method. In contrast, in the latter 30° region, using ON_PWM or H_ON-L_PWM method can result in less torque ripple.

Similarly, in the case of lower bridge current commutation, the difference of torque ripple between ON-PWM (H_PWM-L_ON) and PWM-ON (H_ON-L_PWM) is:

$$\Delta T_2 = \Delta T_{l1} - \Delta T_{l2} = (\frac{\pi}{3} - 2\omega t)\cdot(1-D)\cdot\frac{2k_e n_p U_{dc}t}{\pi L} \tag{29}$$

Same as the upper-bridge current commutation, T_2 yields,

$$\begin{cases} \Delta T_2 \ge 0, & 0 \le \omega t \le \dfrac{\pi}{6} \\ \Delta T_2 < 0, & \dfrac{\pi}{6} < \omega t \le \dfrac{\pi}{3} \end{cases} \tag{30}$$

From equation (30), it can be found that when operating at lower-bridge current commutation, minimum torque ripple appears in the former 30° region by PWM-ON or H_ON-L_PWM method and in the latter 30° region by ON-PWM or H_PWM-L_ON method.

Combining the conclusions above, the new PWM method can be described as: in each operation region of 60° in electrical degrees, torque ripple can be supressed by PWM-ON

TABLE 3. Modulation method with minimum torque ripple.

Region refinement	modulation method with less torque ripple	
	upper-bridge current commutation	lower-bridge current commutation
0°~30°	PWM-ON H_PWM-L_ON	PWM-ON H_ON-L_PWM
30°~60°	ON-PWM H_ON-L_PWM	ON-PWM H_PWM-L_ON

mode in the first 30° region and by ON-PWM mode in the latter 30° region, no matter whether in upper-bridge or lower-bridge current commutations. The new region-refinement PWM mode schematic diagram is shown in Fig. 7.

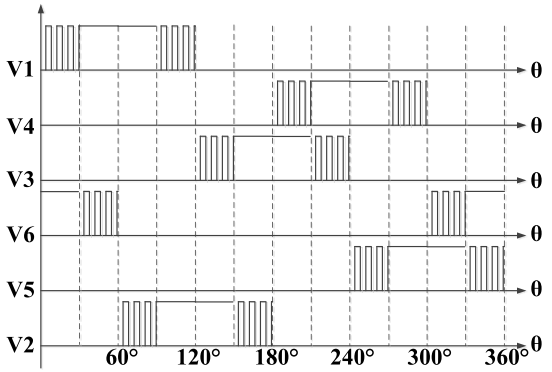

FIGURE 7. New region-refinement PWM mode schematic diagram.

IV. SIMULATIONS AND EXPERIMENTS

To verify the new PWM mode, firstly a simulation is conducted. The key parameters of the BLDCM used in the simulations are listed in Table 4. When the BLDCM goes into steady state (0.10s~0.20s), the phase current waveforms and the torque waveforms under the four PWM modes are shown in Fig. 8. From Fig. 8, it can be seen that current ripples exist during the commutation process under four PWM modes,

TABLE 4. The parameters used in the simulation of the BLDCM.

Parameters	Value	Parameters	Value
R_s (Ω)	3.37	U_{dc} (V)	220
L_s (mH)	20.68	n_p	3
J (kgm2)	0.0018051	n_N (r/min)	780
T_L (NM)	3	k_e (V s/rad)	0.2873

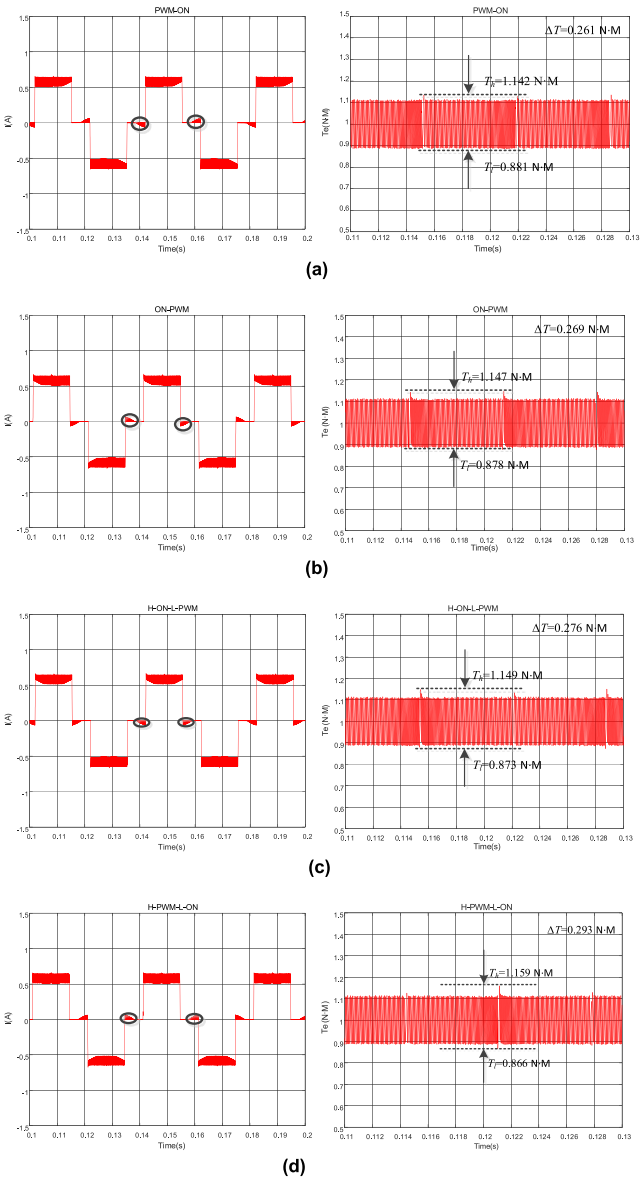

FIGURE 8. Phase current waveforms and torque ripples under traditional four PWM modes. (a) PWM-ON. (b) ON-PWM. (c) H_ON-L_PWM. (d) H_PWM-L_ON.

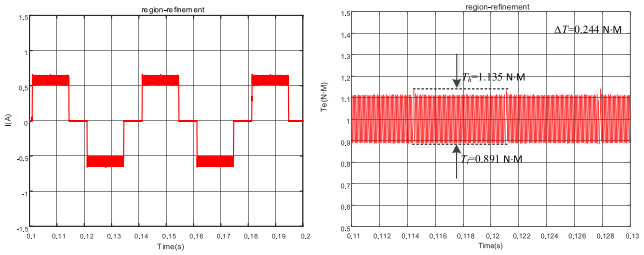

FIGURE 9. Phase current waveforms and torque ripples under the region-refinement mode.

where in Fig. 9, the current pulsation under commutation is negligible by the new PWM mode. Similarly, the pulsation of the torque ripple due to commutation can also be supressed by comparing the torque waveforms in Fig. 8 and Fig. 9.

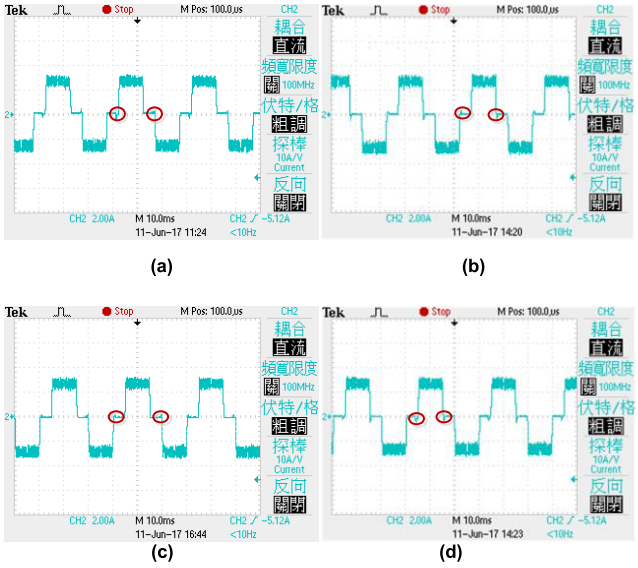

FIGURE 10. Measured phase currents under traditional four PWM modes. (a) PWM-ON. (b) ON-PWM. (c) H_PWM-L_ON. (d) H_ON-L_PWM.

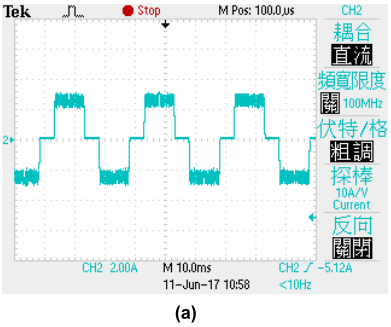

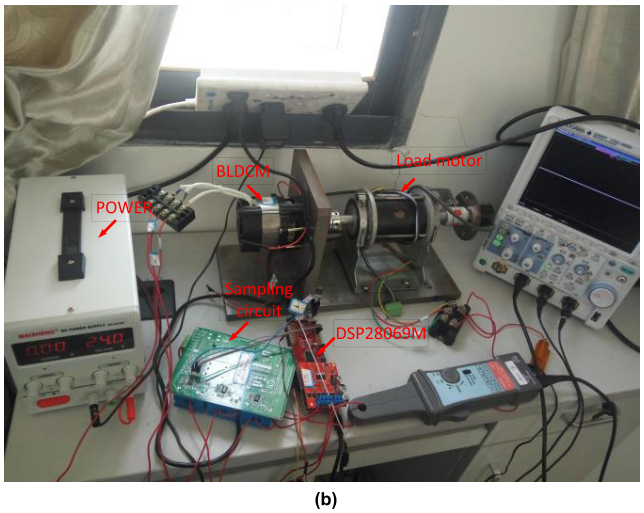

FIGURE 11. Measured phase current under region-refinement PWM mode and the BLDCM-based experimental platform. (a) Measured phase current under region-refinement PWM mode. (b) The BLDCM-based experimental platform.

Further, a prototyped BLDCM-based drive system is setup as shown in Fig. 11(b), where the measured BLDCM has the same parameters as listed in Table 4. TMS320F28069M is used as the core in the control system. The rated voltage of the BLDCM is 24V, the rated power is 200W, and the rated speed is 3000r/min.

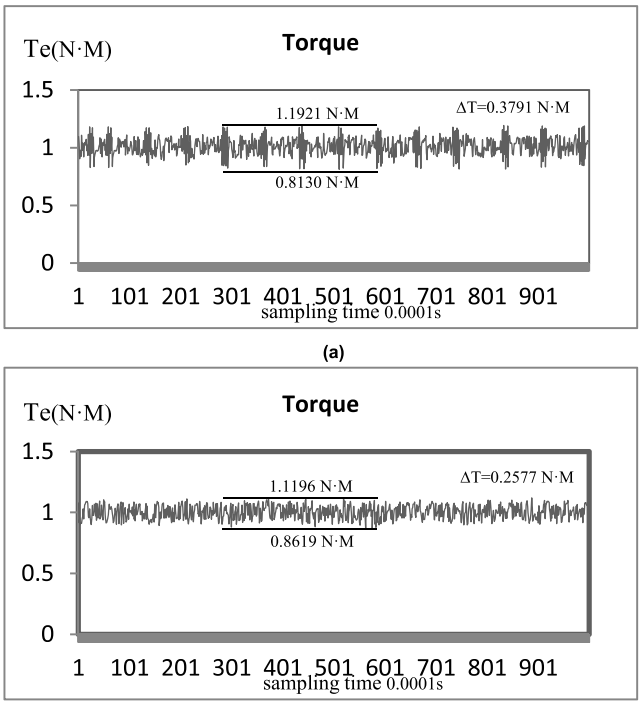

FIGURE 12. Measured torque waveform under different PWM modes. (a) Measured torque waveform under PWM-ON mode. (b) Measured torque waveform under region-refinement PWM mode.

Fig. 10 shows the measured phase current waveforms by four traditional modulation modes. Also, the current ripple can be found as circled out during the commutation region. Fig. 11(a) is the phase current waveform under the new region-refinement modulation with less pulsation.

In term of the torque, the measured torque waveform from a torque sensor under conventional PWM-ON mode is shown in Fig. 12(a), where the torque ripple $\Delta T = 0.3791$N·M as highlighted. However, when the proposed region-refinement mode is applied, the freewheeling current almost disappears as is shown in Fig. 12(b) and the torque ripple is reduced as $\Delta T = 0.2577$Nm, which is evenly distributed during the whole operation region as shown.

V. CONCLUSIONS

To reduce the torque ripple of BLDCM, especially for the pulsation component due to commutation, the influences of typical four PWM modes during commutation on the resultant phase current and consequently the electromagnetic torque, are firstly analyzed and analytical expressions of the torque ripple under each PWM mode is derived. Based on the torque ripple expressions, a new region-refinement PWM mode is proposed for a six-switch-driven BLDCM, which further splits the conventional 60° operation region into the former 30° region and the latter 30° region. In the former

and latter 30° regions, PWM-ON and ON-PWM modulation methods can be employed respectively to reduce the torque ripple. Both simulations and experiments on a prototyped BLDCM verify the effectiveness of the new PWM mode.

APPENDICES

Fig. 1(c) shows the ideal phase back electromotive force (back-EMF) of a BLDCM under a certain speed. If each 60° sector is defined starting from 0° as reference, then three-phase back-EMFs can be calculated as illustrated in Table 5.

TABLE 5. Three-phase back electromotive force (back-EMF) distributions.

Regions	A	B	C
0~π/3	$k_e\omega$	$-k_e\omega$	$-6\ k_e\omega^2t+ k_e\omega$
π/3 ~2π/3	$k_e\omega$	$6\ k_e\omega^2t- k_e\omega$	$-k_e\omega$
2π/3~π	$-6\ k_e\omega^2t+ k_e\omega$	$k_e\omega$	$-k_e\omega$
π~4π/3	$-k_e\omega$	$k_e\omega$	$6\ k_e\omega^2t- k_e\omega$
4π/3~5π/3	$-k_e\omega$	$-6\ k_e\omega^2t+ k_e\omega$	$k_e\omega$
5π/3~2π	$6\ k_e\omega^2t- k_e\omega$	$-k_e\omega$	$k_e\omega$

REFERENCES

[1] X.-J. Zhang and B.-S. Chen, "Influence of PWM modes on commutation torque ripples in sensorless brushless DC motor control system," *J. Shanghai Univ.*, vol. 5, no. 3, pp. 217–223, 2001.
[2] Y. Liu, Z. Q. Zhu, and D. Howe, "Commutation-torque-ripple minimization in direct-torque-controlled PM brushless DC drives," *IEEE Trans. Ind. Appl.*, vol. 43, no. 4, pp. 1012–1021, Jul. 2007.
[3] A. H. Niasar, A. Vahedi, and H. Moghbelli, "Analysis of commutation torque ripple in three-phase, four-switch brushless DC (BLDC) motor drives," in *Proc. 37th IEEE-Power Electron. Spec. Conf.*, Jun. 2006, pp. 1–6.
[4] B.-H. Kang, C.-J. Kim, H.-S. Mok, and G.-H. Choe, "Analysis of torque ripple in BLDC motor with commutation time," in *Proc. IEEE Int. Symp. Ind. Electron.*, vol. 2, Jun. 2001, pp. 1044–1048.
[5] D. R. Hipkins and M. L. Schiedermayer, "Brushless DC motor control system," U.S. Patent 4 208 621, Jun. 17, 1980.
[6] C. Danjiang, L. Zhaoshen, R. Junjun, and Z. Zhongchao, "Analysis of effects on BLDCM torque ripple by PWM modes," *Electr. Drive*, vol. 35, no. 4, pp. 18–20, Apr. 2005.
[7] J.-H. Song and I. Choy, "Commutation torque ripple reduction in brushless DC motor drives using a single DC current sensor," *IEEE Trans. Power Electron.*, vol. 19, no. 2, pp. 312–319, Mar. 2004.
[8] X. J. Zhang and B.-S. Chen, "The different influences of four PWM modes on commutation torque ripples in brushless DC motor control system," *Electr. Mach. Control*, vol. 7, no. 2, pp. 87–91, 2003.
[9] G. Jie and W. Ma, "Research on the pulse-width modulation methods of brushless DC motor taking consideration of commutation," *Trans. China Electrotech. Soc.*, vol. 20, no. 9, pp. 66–71, Sep. 2005.
[10] X. Bao and Y. Zhang, "Analysis of commutation torque ripple of brushless DC motor and its minimization methods," *Small Special Electr. Mach.*, vol. 2, p. 004, Feb. 2007.
[11] R. Carlson, M. Lajoie-Mazenc, and J. C. D. S. Fagundes, "Analysis of torque ripple due to phase commutation in brushless DC machines," *IEEE Trans. Ind. Appl.*, vol. 28, no. 3, pp. 632–638, May 1992.
[12] Z. Xiaofeng and L. Zhengyu, "A new BLDC motor drives method based on BUCK converter for torque ripple reduction," in *Proc. CES/IEEE 5th Power Electron. Motion Control Conf.*, vol. 3, Aug. 2006, pp. 1–4.
[13] T. Shi, Y. Guo, P. Song, and C. Xia, "A new approach of minimizing commutation torque ripple for brushless DC motor based on DC–DC converter," *IEEE Trans. Ind. Electron.*, vol. 57, no. 10, pp. 3483–3490, Oct. 2010.
[14] H. S. Chuang, Y.-L. Ke, and Y. C. Chuang, "Analysis of commutation torque ripple using different PWM modes in BLDC motors," in *Proc. Conf. Rec. IEEE Ind. Commercial Power Syst. Tech. Conf.*, May 2009, pp. 1–6.
[15] M. Liu, H. Guo, and M. Song, "Ripple torque analysis and simulation of BLDC motor with different PWM modes," in *Proc. 7th Int. Power Electron. Motion Control Conf.*, Jun. 2012, pp. 973–977.
[16] W. Kun, R. Junjun, T. Fanghua, and Z. Zhongchao, "A novel PWM scheme to eliminate the diode freewheeling in the inactive phase in BLDC motor," in *Proc. PESC*, vol. 3, Jun. 2004, pp. 2282–2286.
[17] K. Wei, C. Hu, Z. Zhang, and Z. Lu, "A novel commutation torque ripple suppression scheme in BLDCM by sensing the DC current," in *Proc. PESC*, Jun. 2005, pp. 1259–1263.
[18] G. Meng, H. Xiong, and H. Li, "Commutation torque ripple reduction in BLDC motor using PWM_ON_PWM mode," in *Proc. ICEMS*, Nov. 2009, pp. 1–6.
[19] P. H. Tang, Z. H. Liao, and T.-C. Li, "Double-frequency PWM control scheme for BLDCM," *Electr. Mach. Control*, vol. 13, no. 3, pp. 389–397, 2009.
[20] S. Bi, M. Zhou, Z. Gao, and Q. Gu, "Research on torque ripple modulation for permanent brushless DC motor based on DSP," in *Proc. IEEE 7th Int. Power Electron. Motion Control Conf.*, Harbin, China, Jun. 2012, pp. 2516–2521.
[21] H. Li, W. Chou, and Z. Feng, "Analysis and suppression of torque ripple during non-commutation of brushless DC motor," *Micromotors*, vol. 44, no. 4, pp. 1–5, 2011.

KAI LIU received the B.Sc., M.Sc., and Ph.D. degrees in electrical engineering from the Harbin Institute of Technology, Harbin, in 2005, 2007, and 2014, respectively.

Since 2015, he has been with Southeast University, where he is currently a Lecturer with the School of Electrical Engineering. His teaching and research interests include control of electrical machines and flywheel energy storage systems.

ZHIQIANG ZHOU received the B.S. degree in electrical engineering from the Harbin Institute of Technology, Harbin, in 2015, and the M.S. degree in electrical engineering from Southeast University, Nanjing, China, in 2018. His research interests include power converters and modern control of brushless machines.

WEI HUA (M'03–SM'16) received the B.Sc. degree in electrical engineering from the Department of Electrical Engineering, Southeast University, Nanjing, China, in 2001, and the Ph.D. degree in electrical engineering from the School of Electrical and Electronic Engineering, Nanjing, in 2007.

Since 2007, he has been with Southeast University, where he is currently a Professor with the School of Electrical Engineering. His teaching and research interests include the design, analysis, and control of electrical machines, especially for brushless machines, and motor drives for electric vehicles. He has authored or co-authored over 150 technical papers and holds over 50 patents in these areas.